



Short communication

Circular dichroism studies of type III collagen mimetic peptides with anti- or pro-aggregant activities on human platelets

Julien Pêcher^a, Viviane Pires^a, Ibtissem Djaafri^{b,c}, Sophie Da Nascimento^a,
Françoise Fauvel-Lafève^{b,c}, Chantal Legrand^{b,c}, Pascal Sonnet^{a,*}

^a Laboratoire des Glucides, UMR-CNRS 6219, Faculté de Pharmacie, Université de Picardie Jules Verne, 1 rue des louvels, F-80037 Amiens, France

^b INSERM, U553, IFR 105, Paris F-75475, France

^c Université Paris VII, Institut d'Hématologie, Paris F-75475, France

ARTICLE INFO

Article history:

Received 4 April 2008

Received in revised form

14 October 2008

Accepted 20 October 2008

Available online 31 October 2008

Keywords:

Peptide sequence Lys-Hyp-Gly-Glu-Hyp-

Ala-Pro-Lys

CD studies

Left-handed polyproline II conformation

α -Triple-helix peptides

Anti-aggregant and pro-aggregant activities

ABSTRACT

We report the synthesis of collagen related peptides containing the peptide sequence Lys-Hyp-Gly-Glu-Hyp-Gly-Pro-Lys. The anti-thrombotic activity effects of different glycine mutations in this sequence were studied in regard with their different adopted conformations. The biological results could be correlated to the glycine propensity to adopt a more stable polyproline II helix conformation. The incorporation of these sequences in “collagen-like” α -triple-helix peptides shows a pro-thrombotic activity compared to a scrambled negative control peptide which possesses no significant activity.

© 2008 Elsevier Masson SAS. All rights reserved.

1. Introduction

Collagen, which consists of three left-handed polyproline II-like helices supercoiled into a right-handed triple helix, is the main structural component of skin, bone and tendon [1]. The close packing of the three chains requires that Gly occupy every third position, giving a Gly-X-Y repeating sequence. Imino acids stabilize the extended polyproline II nature of the individual chains, and typically about 20% of the X and Y positions are occupied by proline or hydroxyproline (Hyp), respectively. Twenty seven distinct types of human collagens have been identified so far and the most abundant of these are found in characteristic collagen fibrils (major types I, II, III and minor types V and XI) [2]. Vascular type I and III collagens exposed to flowing blood upon vessel wall injury, are among the most thrombogenic components of the subendothelial layer [3]. Platelet interactions with collagens involve different platelet receptors that bind directly or indirectly to collagen fibers [4,5]. The type III Collagen Binding Protein (TIIICBP) is a new receptor for type III collagen [6] which specifically interacts with

the Lys-Hyp-Gly-Glu-Hyp-Gly-Pro-Lys octapeptide **1**. This sequence is located in the CB4 fragment of the type III collagen α 1-chain. This octapeptide **1** inhibits platelet interaction with type III collagen in both static and flow conditions [6,7]. In vivo, the octapeptide **1** prevents photochemically-induced thrombosis in arterioles of mice without affecting bleeding time [8].

We have previously demonstrated that the incorporation of peptide **1** into a more stable β -sheet and β -turn secondary structured peptide leads to an increased capacity for peptide **1** to inhibit type III collagen-induced platelet aggregation. Moreover, the sequence **1** introduced in “collagen-like” α -triple-helix peptides is able to trigger platelet aggregation [9]. In continuation of our work, we present here the results concerning the synthesis, conformational studies and biological activities of type III collagen related peptides containing the mutated sequence **1**. Our goal was first, to study the amino acid roles of **1** in regard with its platelet aggregation inhibiting activity; second, to evaluate the platelet-aggregatory potential of the peptide **1** mutants when incorporated into a α -triple-helix construct mimicking the tertiary and quaternary structures of collagen. For the first purpose, we have studied three octapeptides similar to the peptide **1** with selected amino acid substitutions [10]. To test the second issue, the sequence **1** was flanked with Gly-Pro-Pro sequences at both sides to generate

* Corresponding author. Tel.: +33 322827494; fax: +33 322827469.

E-mail address: pascal.sonnet@u-picardie.fr (P. Sonnet).

covalently-linked (peptide **6**) or spontaneously-formed triple α -helix structures (peptides **7**, **8**).

2. Chemistry

2.1. Synthesis

The synthesis of peptides **1–8** (Graphic 1) was carried out automatically using an applied biosystem 433A. Herein, only the synthesis of the octapeptides **2–4** and **8** is described since the other synthesis description have been already done [9,11]. In the case of peptides **6–8**, further Gly-Pro-Pro triplets were added at each end to allow the adoption of a stable triple-helix conformation. Gly-Pro-Pro triplets were chosen instead of Gly-Pro-Hyp triplets to avoid any recognition by GP VI [12] and to be sure that these peptides **6–8** will specifically interact with TIIICBP. A Gly-Pro-Cys sequence was included at each end to allow cross-linking in order to produce a polymer, since collagen quaternary structure is also essential for the expression of its platelet aggregating activity (fibrillar network).

2.2. Structural studies

The triple-helix conformation was determined for peptides **1–8** by thermal denaturation monitored by CD measurement (Figs. 1–3). These spectroscopic studies were carried out in acetic acid 0.5 M (solvent A) and/or in methanol/acetic acid (85/15) (solvent B) mixture and were equilibrated at least one week before measurements [13]. Peptide solutions of concentration 1 mg/mL were used, with peptides dried *in vacuo* over P_2O_5 for 48 h prior to weighing.

2.2.1. Peptides 1–4

Peptides **2** and **3** are closed to peptide **1**. In the case of peptide **2**, one glycine was substituted by an alanine while in the peptide **3** the two glycines were substituted by two alanines. The peptide **4** is supposed to be a negative octapeptide control without any thrombotic activity in which the eight amino acids are found in a random sequence.

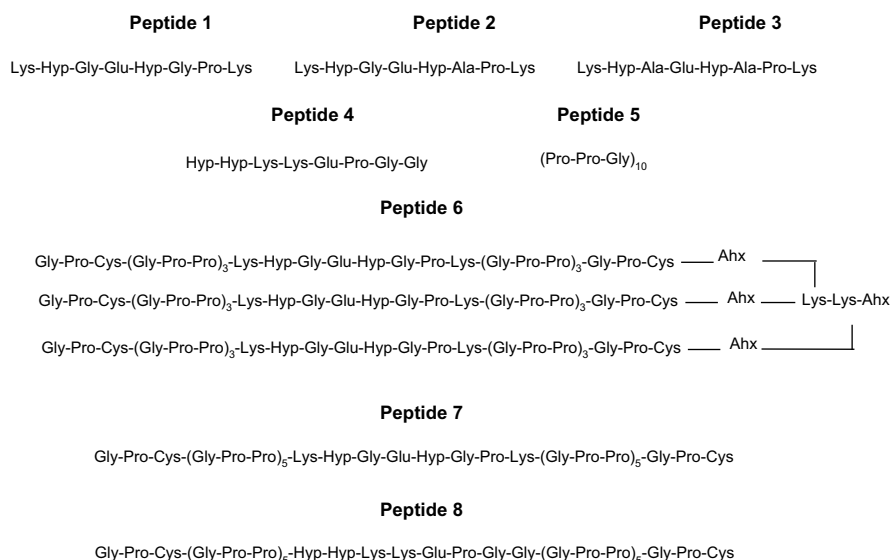
In solvent A (Fig. 1A), CD spectra of peptides **1** and **2** have a strong negative band at 194 nm and a weaker positive band at 220 nm. Such spectra are characteristics of a left-handed polyproline II (P_{II}) conformation since the P_{II} helix is the only secondary

structure known to have a positive band around 218–228 nm [13]. The peptide **3** spectrum presents a negative large band at 190 nm and positive large band at 222 nm. As the intensity of the positive band is taken to be proportional to the P_{II} helical content, this peptide **3** spectrum can indicate an increase in the P_{II} helical content compared to the peptides **1** and **2**. While the peptide **4** spectrum possesses only a strong negative band at 220 nm which is characteristic of a random coil conformation and not to a P_{II} structure as the negative band doesn't decrease when the temperature is increased [14].

These four peptides **1–4** were also examined to answer the question of what happens to the P_{II} content in the presence of solvent B since methanol, known to stabilize triple-helical structures [15], was used as co-solvent in order to amplify and detect possible weak triple-helical or polyproline II propensities. The intensities of the bands in the CD spectrum for the peptide **4** are similar to those obtained in solvent A, corresponding to a random coil conformation too (Fig. 1B). In solvent B, the peptide **1** spectrum indicates an increase of the positive band with a decreased of the negative band which is characteristic of an increase of the P_{II} helix conformation. For the peptide **2** spectrum, the intensities of the bands change in an opposite manner to those observed for the peptide **1** spectrum which is due to an increase of the other secondary or random coil conformation structures. For the peptide **3** spectrum, the negative and positive band diminutions, indicate a P_{II} helix conformation decrease. In the case of the peptide **1**, solvent B reinforces the P_{II} conformation while in the other alanine based peptides **2** and **3**, the same solvent seems to reinforce the proportion of the other secondary or random coil structures which are found in these two peptides [16].

2.2.2. Peptides 5–8

In order to investigate the triple-helical profiles of our synthetic collagen-based peptides **5–8**, their CD spectra were determined (Fig. 2). In solvent A, these spectra exhibit a large negative peak around 200 nm and small positive peak around 225 nm (Fig. 2A), which are characteristics of collagen-like triple-helical or P_{II} -like structures. In solvent B CD spectra (Fig. 2B), the increase of intensities of the positive and negative band are in agreement with the methanol propensity to stabilize helical structures [15] which can be very useful to amplify and detect very weak triple-helical propensities [15,17]. The parameter R_{pn} [17] value which is related



Graphic 1. Structure of peptides **1–8**.

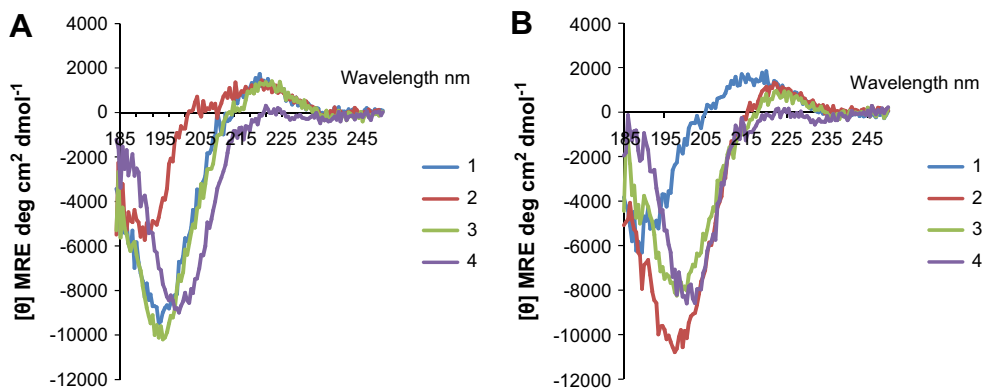


Fig. 1. (A) CD spectra in acetic acid 0.5 M of **1** (blue, 1 mg/mL), **2** (chestnut, 1 mg/mL), **3** (green, 1 mg/mL) and **4** (purple, 1 mg/mL) at 4 °C; (B) CD spectra in a mixture of methanol and acetic acid (85/15) of **1–4** at 4 °C. (For interpretation of the references to color in this figure legend, the reader is referred to the web version of this article).

to the CD peak intensities was found to be useful in establishing triple-helical conformations in solution. The peptide **5** triple-helical conformation is well known [18]. From Table 1, it can be seen that the R_{pn} values for our peptides **6–8** are essentially the same as the R_{pn} value exhibited by peptide **5** (R_{pn} near 0.1, solvent B). These results are consistent with a collagen-like triple-helical structure for the peptides **5–8**. In addition, the percentages of P_{II} structures are always found higher in solvent B conditions and are close to the peptide **5** percentage value.

Measurements of the CD molar ellipticity (θ) as a function of temperature have been used to monitor the thermal denaturation of the peptides **5–8**. The melting curves obtained by optical rotation measurements in solvent B are presented in Fig. 3A. The temperature where the peptide was 50% folded ($F=0.5$) was taken as the melting temperature (T_m) as shown in Fig. 3B. The peptide T_m values obtained in solvent B (Table 1) are contained between 33.3 °C and 41.4 °C. These values indicated a good thermal stability of these peptides. The T_m of peptides **7** and **8** are, respectively, 40 °C and 33 °C. The decrease in melting temperature for **8** shows the significant effect of the incorporation of the random coil octapeptide **4** on triple-helical conformation. Incorporation of the octapeptide **1** in the template-assembled synthetic peptide **6** didn't lead to a more stable triple-helical conformation ($T_m=33.9$ °C) compared to the spontaneously-formed triple-helix structure peptide **7** ($T_m=40.8$ °C). The van't Hoff enthalpy (ΔH_{vH}) and entropy (ΔS) for the peptides **5–8** were determined from the thermal equilibrium curves assuming a two-state monomer to trimer transition. The concentrations used for calculating the thermodynamic parameters were taken from weighing since the differences in concentration from amino acid analysis vs weighing

had no effect on the enthalpy values and little effect on ΔS (<1%) and ΔG (<3%) determination [19]. The ranking of their relative free energy values calculated is consistent with the order of their observed thermal stabilities (Table 1). The same triple-helical conformation for these four peptides allowed us to establish a stability scale by calculation of the $\Delta\Delta G$ values. Comparison of thermodynamics parameters indicates that the incorporation of the random coil octapeptide **4** in the collagen-like triple-helical peptide **8** decreases the stability as a result of a less favorable enthalpy term.

3. Pharmacology

3.1. Platelet aggregation assay

Human blood was taken from the antecubital vein of healthy volunteers not taking any medication, and directly added into 3.8% sodium citrate (1:9 v/v blood). Blood was centrifuged for 15 min at 150 g to obtain Platelet Rich Plasma (PRP). PRP was harvested and centrifuged for 15 min at 1.200 g. Platelets pellets were then resuspended in pH 6.5 Patcheke's buffer (36 mM citric acid, 5 mM glucose, 5 mM KCl, 2 mM CaCl_2 , 1 mM MgCl_2 , 103 mM NaCl) containing 0.1 μM PGE_1 washed once and resuspended in pH 7.5 Tyrode's buffer (137 mM NaCl, 2.7 mM KCl, 1.2 mM NaHCO_3 , 0.36 mM NaH_2PO_4 , 2 mM CaCl_2 , 1 mM MgCl_2 , 5 mM HEPES, 5.5 mM glucose) and adjusted at 2×10^8 platelets/mL. Platelet aggregation was monitored by measuring light transmission through the stirred suspension of washed platelets using a Beckman Chrono-Log aggregometer. In the present study, washed platelet conditions were consciously chosen to ascertain that the inhibiting effect of the peptides was on collagen III-induced platelet aggregation solely

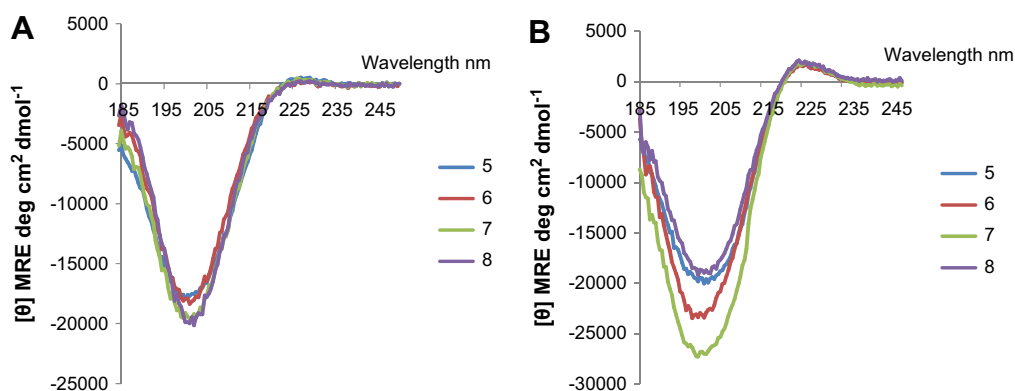


Fig. 2. (A) CD spectra in acetic acid 0.5 M of **5** (blue, 1 mg/mL), **6** (chestnut, 1 mg/mL), **7** (green, 1 mg/mL) and **8** (purple, 1 mg/mL) at 4 °C; (B) CD spectra in a mixture of methanol and acetic acid (85/15) of **5–8** at 4 °C. (For interpretation of the references to color in this figure legend, the reader is referred to the web version of this article).

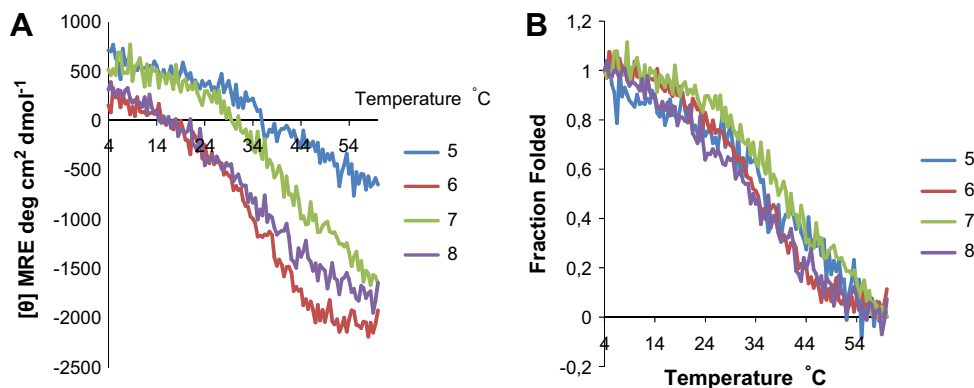


Fig. 3. Thermal equilibrium curves of peptides **5**, **6**, **7**, **8** in methanol/acetic acid (85/15), showing their sharp transitions and the variations in thermal stability. (A) Mean residue ellipticity $[\theta]$ vs temperature; (B) fraction folded vs temperature.

and not due to a side effect of peptides on other activating, or amplifying, pathways dependent on plasma components such as fibrinogen, von Willebrand factor or thrombin activation.

We have previously reported that the peptide **1** inhibits type III collagen-induced human platelet aggregation [8]. Herein, the peptides **1–4** are tested (in triplicates at least) on the human platelets, platelet aggregation being induced by 10 $\mu\text{g}/\text{mL}$ of human type III collagen. Fig. 4 is a representative figure from experiments done in triplicate, all showing similar and significant differential inhibitory responses between peptide **1** and peptides **3–4**. At peptide concentration of 1 mM, Peptide **1** inhibited by $86.1 \pm 0.1\%$ type III collagen-induced human platelet aggregation. Peptide **2** had a similar effect ($72.1 \pm 0.2\%$ of inhibition). When comparing peptides **3** and **4** to peptide **1**, the peptides **3** and **4** do not possess any inhibitory effect on human platelet aggregation (Fig. 4). The collagen-like triple-helix peptides **6** and **7** supported, in a moderate but significant way, platelet aggregation [9]. Peptide **8** at a concentration of 500 $\mu\text{g}/\text{mL}$ did not induce a platelet aggregation compared to peptide **6** at the same concentration (Fig. 5).

4. Discussion

Type III collagen is the most thrombogenic component of the subendothelial layer together with type I collagen [3]. Type III collagen possesses repetitive sequence patterns that promote regular spatial.

Table 1

Thermodynamics parameters ΔH (kJ mol^{-1}), ΔS ($\text{J mol}^{-1} \text{K}^{-1}$), ΔG (kJ mol^{-1}), together with the observed melting temperatures (T_m) and structural data (P_{II} percentage, R_{pn}) corresponding to the transition coil \leftrightarrow triple helix in solvent A (0.5 M acetic acid) or B (methanol/acetic acid: 85/15) for the collagen-like triple-helical peptides **5–8**.

Peptide	Solvent	T_m ($^{\circ}\text{C}$)	ΔH	ΔS	ΔG	$\Delta\Delta G$	% P_{II}	R_{pn}
5	A	ND	ND	ND			48	0.03
	B	41.4	−189	−471.8	−42.51	0.00	59	0.1
6	A	ND	ND	ND			46	0.01
	B	33.9	−157	−511.1	1.68	−40.83	57	0.07
7	A	ND	ND	ND			48	0.03
	B	40.8	−192	−471.9	−45.48	2.97	58	0.07
8	A	ND	ND	ND			46	0.01
	B	33.2	−86	−258	−5.89	−36.62	60	0.1

^a ΔH was calculated from the equilibrium melting transition using the van't Hoff equation (see Section 5.3.2). Using this value of ΔH , ΔS was calculated at T_m . The average of the melting temperatures for peptides **5–8** ($T = 310.4 \text{ K}$) was used for the calculation of ΔG .

^b $\Delta\Delta G$ (kJ mol^{-1}) values are given here for each peptide relative to the peptide **5**.

^c R_{pn} represents the ratio of positive peak intensity over negative peak intensity (absolute values).

ϕ and ψ angles of constituent residues are restricted to around -75° and $+145^{\circ}$, respectively. Most P_{II} helices are shorter than five residues, although the longest found contained 12 amino acids. P_{II} helices are highly solvent exposed, which explains why apolar amino acids are disfavoured [20]. Alanine possesses a high propensity to adopt the P_{II} helical structure [16]. Backbone–backbone hydrogen bonds were excluded from the survey of protein P_{II} helices, so these residues are hydrogen bonded to solvent, to side chains [20]. Kelly and coll. have proposed that backbone–solvent interactions are an important component of observed propensities [21].

The goal of our study was first to better understand how the amino acid sequence of the peptide **1** (CB4 fragment of the type III collagen α -1 chain) determines the secondary structure in regard with its human platelet aggregation inhibitory activity. Doing so, we have studied two octapeptides with selected one (peptide **2**) or two glycine(s) (peptide **3**) substitutions and a scrambled negative

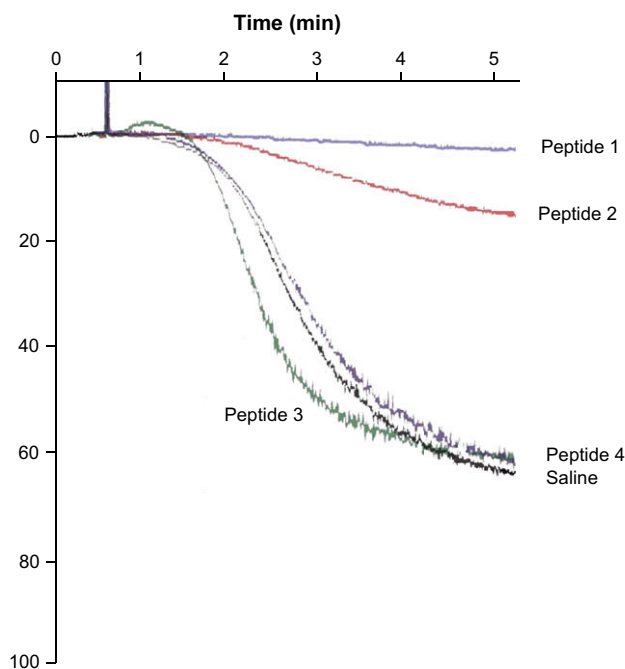


Fig. 4. Inhibitory effects of 1 mM of peptide **1** (purple tracing), peptide **2** (red tracing), peptide **3** (blue tracing), peptide **4** (green tracing) on human platelet aggregation induced by type III collagen. As control platelet aggregation was induced by type III collagen alone (black tracing). (For interpretation of the references to color in this figure legend, the reader is referred to the web version of this article.)

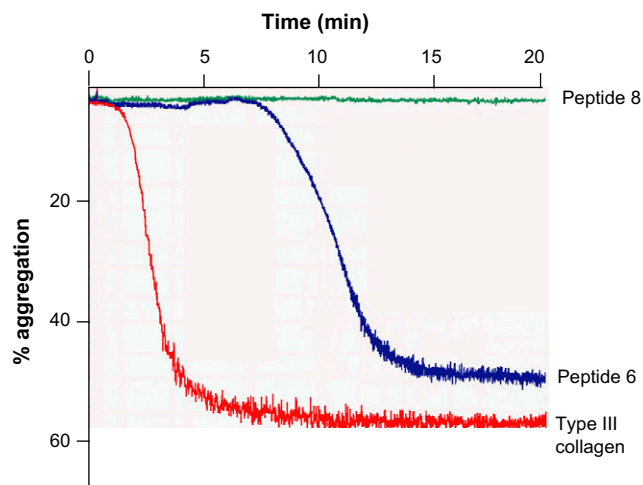


Fig. 5. Platelet aggregation induced by collagen-like triple-helix: peptide **6** (blue tracing) or peptide **8** (green tracing) were added (500 $\mu\text{g/mL}$) to washed platelets in the aggregometer's basin. As control, platelet aggregation was induced by 10 $\mu\text{g/mL}$ of type III collagen. (For interpretation of the references to color in this figure legend, the reader is referred to the web version of this article).

control peptide **4**. The choice of these substitutions is based on the structural requirements studies of the Lys-Pro-Gly-Glu-Pro-Gly-Pro-Lys peptide previously established by Erickson and coll. [10]. They have demonstrated that substitutions which led to the reduction of the β -turn potential significantly reduced the inhibitory activity of the corresponding peptides. Since, the dihedral angles for a structure of the P_{II} helix type and a structure of the β -turn type are very near, it could be postulated, in the case of the octapeptides **1–4**, that a decrease of P_{II} conformation is correlated to a decrease of the platelet aggregation inhibitory activity. Contrary to the peptide **1** CD study, the peptides **2–3** CD studies have indicated a P_{II} helix conformation decrease in solvent B. The solvent B conditions reinforce the proportion of the other secondary or random coil structures which are found in these two peptides. Indeed, the backbone of the alanine residue is well-exposed to solvent in the P_{II} helix conformation of the peptides **2** and **3**, allowing the formation of multiple hydrogen bonds with water molecules (solvent A), contributing to the stability of the P_{II} helical content observed. In contrast, methanol (solvent B) prevents water hydrogen bonding leading to a P_{II} helix conformation decrease as observed for the same peptides **2** and **3** [21,22].

Concerning the peptide **4**, a random coil conformation was found in the two experimental condition CD studies. These results have shown that only peptides **1** and **2** presented a strong degree of P_{II} proportion. As a result, we have shown that the two peptides **3** and **4** didn't possess any platelet aggregation inhibitory activity compared to the peptides **1** and **2**. Two glycine mutations (peptide **3**) or a random conformation (peptide **4**) have a destabilizing effect of the P_{II} helix conformation leading to a decrease of the platelet aggregation inhibitory activity.

A second goal was to analyze the structural requirements for the pro-aggregating activity of derived peptides. We have studied three collagen-like triple-helical peptides **6–8** which incorporated the sequence **1** or the scrambled sequence **4**. A poly(proline)-based host was chosen since such peptides are known to form stable P_{II} helices in aqueous solutions. Feng et al. [17] have demonstrated that at least five repeats of the collagen Gly-Pro-Hyp are required for significant trimer formation (peptides **7** and **8**). Three octapeptides **1** have been linked, via two consecutively connected lysine residues with three functional groups, to a "collagen-like" α -triple-helical peptide **6**. Fields and coll. have demonstrated that this template possessed a stabilizing effect on the collagen-like triple-helical structures [2b,11].

The CD studies have shown that the three peptides **5–8** are structured in "collagen-like" α -triple-helix. Thermodynamic parameters provide a basis for calculation of $\Delta\Delta G$ values for a scale of triple-helix potential. In our case, the poly(proline)-based peptide **7** is more stable than the covalently-linked α -triple-helix peptide **6**. The significant $\Delta\Delta G$ and the 7 $^{\circ}\text{C}$ T_m value differences calculated between peptides **7** and **8** compared to peptide **5** are consistent with the incorporation of the central P_{II} helix sequence **1** or random coil sequence **4**. The lower stability of the peptide **8** could be explained by a lower P_{II} conformation due to the two neighboring side chain lysine electrostatic repulsion of the sequence **4**. In our previous work, we have demonstrated that the sequence **1** introduced in "collagen-like" α -triple-helix peptide **6–7** is able to trigger platelet aggregation [9]. Herein, no platelet aggregation was observed with the peptide **8** incorporating the random coil sequence **4** (Fig. 5). These biological results could be correlated to the thermodynamics parameters which indicate that the incorporation of the random coil octapeptide **4** in the collagen-like triple-helical peptide **8** decreases the stability as a result of a less favorable enthalpy term.

Platelets have several proteins that promote their adhesion to collagen. The sequence **1** represents a domain within CB4 type III collagen $\alpha 1$ chain that specifically interacts with TIIICBP [6]. In this report, the mutation of one or two glycine(s) by the corresponding alanine(s) leads to loss of the anti-thrombotic activity. These biological results could be correlated to the glycine propensity to adopt a more stable P_{II} helix conformation. Melting studies have shown that the incorporation of the random coil sequence **4** forms less stable "collagen-like" α -triple-helix peptide **8** with the loss of the pro-thrombotic activity initially observed for the peptides **6–7**. These results show the importance of the peptide **1** amino acid conformation in the specifically TIIICBP recognition.

5. Experimental section

5.1. Chemistry

High-resolution electrospray mass spectra in the positive ion mode were obtained on a Q-TOF Ultima Global hybrid quadrupole/time-of-flight instrument (Waters-Micromass, Manchester, U.K.), equipped with a pneumatically assisted electrospray (Z-spray) ion source and an additional sprayer (Lock Spray) for the reference compound. The source and desolvation temperatures were kept at 80 and 150 $^{\circ}\text{C}$, respectively. Nitrogen was used as the drying and nebulizing gas at flow rates of 350 and 50 L/h, respectively. The capillary voltage was 3 kV, the cone voltage 100 V and the RF lens1 energy was optimised for each sample (30–150 V). Lock mass correction, using appropriate cluster ions of an orthophosphoric acid solution (0.1% in 50/50 acetonitrile/water) or of a sodium iodide solution (2 mg/ μL in 50/50 propan-2-ol/water + 0.05 mg/ μL caesium iodide), was applied for accurate mass measurements. The mass range was typically 50–2050 Da and spectra were recorded at 2 s/scan in the profile mode at a resolution of 10,000 (FWMH). Data acquisition and processing were performed with MassLynx 4.0 software. Infrared spectra (IR) were recorded on a Jasco FT/IR 4200. Nuclear magnetic resonance (^1H and ^{13}C NMR) spectra were recorded on a BRUKER AVANCE 500 spectrometer (500 MHz) and tetramethylsilane (TMS) was used as an internal standard. ^1H NMR analyses were obtained at 500 MHz (s: singlet, d: doublet, t: triplet, dd: double doublet, m: multiplet), whereas ^{13}C NMR analyses were obtained at 125 MHz. The chemical shifts (δ) are given in parts per million relative to TMS ($\delta = 0.00$).

5.2. General procedure for preparation of **2–4** and **8**

Fmoc(9-fluorophenylmethoxy)-amino acids and Fmoc-amino acids-Sasrin were purchased from Bachem (Germany). The other

chemicals compounds were purchased from Sigma–Aldrich and used without further purification. The peptides were synthesized on an Applied Biosystems Model 433A Peptide Synthesizer, using standard automated continuous-flow solid-phase peptide synthesis methods. Sasrin resin was selected for the synthesis of the protected peptides because protected peptides can be cleaved from the resin with diluted acid solution. Ten-fold molar excess of the above amino acids were used in a typical coupling reaction. Fmoc-deprotection was accomplished by treatment with 20% (v/v) piperidine in *N*-methyl-2-pyrrolidone (NMP). The coupling reaction was achieved by treatment with 2-(1*H*-benzotriazol-1-yl)-1,1,3,3-tetramethyluronium hexafluorophosphate (HBTU) and *N*,*N*-diisopropylethylamine (DIEA) in NMP using a standard Fast-Moc protocol. The peptides were cleaved and side chain deprotected by treatment of the peptide resin with water/thioanisole/triisopropylsilane/dichloromethane/trifluoroacetic acid (1:1:1:10:20 v/v) or with dichloromethane/trifluoroacetic acid (1:9 v/v) for 3–4 h at room temperature. The peptides were purified on an RP-HPLC C18 column (Prosphere® C18, 100 Å 15 µm, 25 × 100 mm) using a mixture of aqueous 0.1% (v/v) TFA (A) and 0.1% (v/v) TFA in acetonitrile/water mixture (80/20, v/v) (B) as the mobile phase (flow rate of 3 mL/min) and employing UV detection at 220 nm. The purity of all peptides was found to be >95%. Electrospray mass spectrometric sequence analysis has been used to confirm the correct sequences (MS-MS, *m/z*).

5.2.1. Lys-Hyp-Gly-Glu-Hyp-Ala-Pro-Lys (2)

The peptide resin NH₂-Lys(Boc)-Hyp(tBu)-Gly-Glu(tBu)-Hyp(tBu)-Ala-Pro-Lys(Boc)-Sasrin®, obtained from commercially available Fmoc-Lys(Boc)-Sasrin® (172.19 mg, 0.103 mmol), was cleaved from the resin and side chain deprotected by treatment with a mixture of dichloromethane/trifluoroacetic acid (1:9 v/v) for 3 h at room temperature. The solid support was removed by filtration, the filtrate concentrated under reduced pressure, and the peptide **2** precipitated from diethyl ether. Precipitate was washed several times with diethyl ether and dried under reduced pressure. Its composition was verified by electrospray mass spectrometric sequence analysis. Peptide **2** was obtained as a white powder (102.74 mg, 89.2%). IR (cm⁻¹): 3318 (COOH, OH), 2940 (NH), 1716 (CO), 1661 (CO). ¹H NMR (500 MHz, CD₃OD), δ (ppm): 1.40 (d, ²*J* = 7.0 Hz, 3H, CH₃, Ala), 1.48 (m, 2H, CH₂γ, Pro), 1.62 (m, 2H, CH₂β, Lys), 1.70 (m, 2H, CH₂γ, Glu), 1.73 (m, 2H, CH₂β, Glu), 1.76 (m, 2H, CH₂γ, Lys), 1.90 (m, 2H, CH₂β, Pro), 1.99 (m, 2H, CH₂β, Hyp), 2.01 (m, 4H, CH₂γ, Lys), 2.03 (m, 2H, CH₂β, Lys), 2.31 (m, 2H, CH₂β, Hyp), 2.43 (m, 4H, CH₂δ, Lys), 2.98 (m, 4H, CH₂ε, Lys), 3.10 (m, 2H, CH₂, Gly), 3.65 (m, 1H, CH₂δ, Pro), 3.77 (m, 2H, CH₂δ, Hyp), 3.79 (m, 1H, CH₂δ, Pro), 3.82 (m, 2H, CH₂δ, Hyp), 4.33 (t, ²*J* = 6.3 Hz, 1H, CHα, Lys), 4.43 (m, 1H, CHα, Hyp), 4.40 (m, 1H, CHα, Lys), 4.49 (m, 1H, CHγ, Hyp), 4.55 (m, 1H, CHα, Pro), 4.56 (m, 1H, CHα, Ala), 4.58 (m, 1H, CHγ, Hyp), 4.59 (m, 1H, CHα, Hyp), 4.83 (m, 1H, CHα, Glu), 7.87 (d, ²*J* = 8.3 Hz, 1H, NH), 8.36 (d, ²*J* = 7.7 Hz, 1H, NH), 8.42 (d, ²*J* = 6.4 Hz, 1H, NH), 8.97 (t, ²*J* = 6.4 Hz, 1H, NH₂). ¹³C NMR (125 MHz, CD₃OD), δ (ppm): 15.2 (CH₃, Ala), 20.6 (CH₂γ, Pro), 22.3 (CH₂β, Lys), 24.5 (CH₂β, Lys), 26.4 (CH₂β, Glu), 26.6 (CH₂γ, Glu), 29.1 (CH₂δ, Lys), 29.3 (CH₂δ, Lys), 29.6 (CH₂β, Pro), 30.6 (CH₂γ, Lys), 37.5 (CH₂β, Hyp), 38.8 (CH₂ε, Lys), 39.2 (CH₂, Gly), 42.2 (CH₂δ, Pro), 47.5 (CHα, Ala), 50.2 (CHα, Glu), 51.3 (CHα, Lys), 51.6 (CHα, Lys), 55.4 (CH₂δ, Hyp), 55.7 (CH₂δ, Hyp), 58.8 (CHα, Pro), 59.8 (CHα, Hyp), 60.0 (CHα, Hyp), 69.5 (CHγ, Hyp), 69.7 (CHγ, Hyp), 167.9 (CO, Lys), 169.8 (CO, Gly), 170.8 (CO, Glu), 171.9 (CO, Ala), 172.2 (CO, Pro), 173.0 (CO, Hyp), 173.6 (COOH, Glu), 175.5 (COOH, Lys). HRMS (ESI-MS, *m/z*) (M + H)⁺ calc. for C₃₇H₆₃N₁₀O₁₃: 855.4576, found: 855.4570.

5.2.2. Lys-Hyp-Ala-Glu-Hyp-Ala-Pro-Lys (3)

The peptide resin NH₂-Lys(Boc)-Hyp(tBu)-Ala-Glu(tBu)-Hyp(tBu)-Ala-Pro-Lys(Boc)-Sasrin®, obtained from commercially

available Fmoc-Lys(Boc)-Sasrin® (173.63 mg, 0.104 mmol), was cleaved from the resin and side chain deprotected by treatment with a mixture of dichloromethane/trifluoroacetic acid (1:9 v/v) for 3 h at room temperature. The solid support was removed by filtration, the filtrate concentrated under reduced pressure, and the peptide **3** precipitated from diethyl ether. Precipitate was washed several times with diethyl ether and dried under reduced pressure. Its composition was verified by electrospray mass spectrometric sequence analysis. Peptide **3** was obtained as a white powder (113.10 mg, 87.2%). IR (cm⁻¹): 3316 (COOH, OH), 2944 (NH), 1713 (CO), 1658 (CO). ¹H NMR (500 MHz, CD₃OD), δ (ppm): 1.38 (m, 6H, CH₃, Ala), 1.58 (m, 2H, CH₂γ, Pro), 1.58 (m, 1H, CH₂β, Lys), 1.65 (m, 1H, CH₂β, Lys), 2.01 (m, 2H, CH₂β, Lys), 1.71 (m, 2H, CH₂β, Glu), 1.75 (m, 2H, CH₂γ, Lys), 1.81 (m, 2H, CH₂γ, Glu), 1.95 (m, 2H, CH₂β, Pro), 2.02 (m, 2H, CH₂γ, Lys), 2.02 (m, 2H, CH₂β, Hyp), 2.20 (m, 2H, CH₂δ, Lys), 2.25 (m, 2H, CH₂β, Hyp), 2.45 (m, 2H, CH₂δ, Lys), 3.65 (m, 2H, CH₂δ, Pro), 2.99 (m, 4H, CH₂ε, Lys), 3.66 (m, 2H, CH₂δ, Hyp), 3.82 (m, 2H, CH₂δ, Hyp), 3.83 (m, 2H, CH₂δ, Pro), 4.32 (m, 1H, CHα, Lys), 4.32 (m, 1H, CHα, Ala), 4.41 (m, 1H, CHα, Lys), 4.45 (m, 1H, CHα, Hyp), 4.52 (m, 2H, CHγ, Hyp), 4.56 (m, 1H, CHα, Pro), 4.61 (m, 1H, CHα, Ala), 4.65 (m, 1H, CHα, Hyp), 4.75 (m, 1H, CHα, Glu), 5.60 (br s, 1H, NH, Ala), 5.70 (br s, 1H, NH, Ala), 8.00 (d, 1H, ²*J* = 1.5 Hz, NH), 8.30 (br s, 1H, NH). ¹³C NMR (125 MHz, CD₃OD), δ (ppm): 15.3 (CH₃, Ala), 16.0 (CH₃, Ala), 20.4 (CH₂γ, Pro), 22.2 (CH₂β, Lys), 24.5 (CH₂β, Lys), 26.3 (CH₂β, Glu), 26.6 (CH₂γ, Glu), 28.4 (CH₂δ, Lys), 29.1 (CH₂β, Pro), 30.3 (CH₂γ, Lys), 30.6 (CH₂γ, Lys), 37.4 (CH₂β, Hyp), 37.7 (CH₂β, Hyp), 38.8 (CH₂ε, Lys), 39.2 (CH₂ε, Lys), 47.0 (CH₂δ, Pro), 49.4 (CHα, Ala), 50.3 (CHα, Glu), 51.3 (CHα, Lys), 51.6 (CHα, Lys), 55.3 (CH₂δ, Hyp), 55.4 (CH₂δ, Hyp), 58.7 (CHα, Pro), 59.0 (CHα, Hyp), 60.0 (CHα, Hyp), 69.5 (CHγ, Hyp), 69.7 (CHγ, Hyp), 167.6 (CO, Lys), 170.8 (CO, Glu), 171.9 (CO, Ala), 172.2 (CO, Ala), 172.3 (CO, Pro), 173.0 (CO, Hyp), 173.2 (CO, Hyp), 173.5 (COOH, Glu), 175.0 (COOH, Lys). HRMS (ESI-MS, *m/z*) (M + H)⁺ calc. for C₃₈H₆₅N₁₀O₁₃: 869.4733, found: 869.4693.

5.2.3. Hyp-Hyp-Lys-Lys-Glu-Pro-Gly-Gly (4)

The peptide resin H₂N-Hyp(tBu)-Hyp(tBu)-Lys(Boc)-Lys(Boc)-Glu(tBu)-Pro-Gly-Gly-Sasrin®, obtained from commercially available Fmoc-Gly-Sasrin® (166.56 mg, 0.114 mmol), was cleaved from the resin and side chain deprotected by treatment with a mixture of dichloromethane/trifluoroacetic acid (1:9 v/v) for 3 h at room temperature. The solid support was removed by filtration, the filtrate concentrated under reduced pressure, and the peptide **4** precipitated from diethyl ether. Precipitate was washed several times with diethyl ether and dried under reduced pressure. Its composition was verified by electrospray mass spectrometric sequence analysis. Peptide **4** was obtained as a white powder (86.68 mg, 81.2%). IR (cm⁻¹): 3338 (COOH, OH), 2950 (NH), 1720 (CO), 1665 (CO). ¹H NMR (500 MHz, D₂O), δ (ppm): 1.47 (m, 2H, CH₂γ, Pro), 1.60 (m, 2H, CH₂β, Lys), 2.15 (m, 2H, CH₂β, Lys), 1.70 (m, 2H, CH₂β, Glu), 1.77 (m, 2H, CH₂γ, Glu), 1.78 (m, 2H, CH₂γ, Lys), 1.87 (m, 2H, CH₂β, Pro), 2.12 (m, 2H, CH₂β, Hyp), 2.22 (m, 2H, CH₂γ, Lys), 2.30 (m, 2H, CH₂β, Hyp), 2.48 (m, 2H, CH₂δ, Lys), 2.61 (m, 2H, CH₂δ, Lys), 3.60 (m, 2H, CH₂δ, Pro), 3.00 (m, 4H, CH₂ε, Lys), 3.84 (m, 1H, CH₂, Gly), 3.86 (m, 1H, CH₂, Gly), 4.10 (m, 1H, CH₂, Gly), 4.12 (m, 1H, CH₂, Gly), 3.60 (m, 2H, CH₂δ, Hyp), 3.61 (m, 2H, CH₂δ, Pro), 3.72 (m, 2H, CH₂δ, Hyp), 4.30 (m, 1H, CHα, Lys), 4.40 (m, 1H, CHα, Lys), 4.40 (m, 1H, CHα, Hyp), 4.49 (m, 1H, CHα, Pro), 4.53 (m, 1H, CHα, Hyp), 4.55 (m, 1H, CHγ, Hyp), 4.70 (m, 1H, CHα, Glu), 4.75 (m, 1H, CHγ, Hyp). ¹³C NMR (125 MHz, D₂O), δ (ppm): 21.9 (CH₂γ, Pro), 22.1 (CH₂β, Lys), 24.8 (CH₂β, Lys), 26.4 (CH₂β, Glu), 26.5 (CH₂γ, Glu), 29.4 (CH₂δ, Lys), 30.0 (CH₂β, Pro), 30.1 (CH₂γ, Lys), 30.5 (CH₂γ, Lys), 36.7 (CH₂β, Hyp), 37.3 (CH₂β, Hyp), 39.9 (CH₂ε, Lys), 41.1 (CH₂, Gly), 42.4 (CH₂, Gly), 48.1 (CH₂δ, Pro), 50.5 (CHα, Glu), 53.2 (CHα, Lys), 53.7 (CHα, Lys), 53.7 (CH₂δ, Hyp), 55.4 (CH₂δ, Hyp), 58.1 (CHα, Pro), 59.1 (CHα, Hyp), 60.5 (CHα, Hyp), 69.9 (CHγ, Hyp), 70.1 (CHγ, Hyp), 171.7 (CO, Lys), 171.9 (CO, Lys), 173.1 (CO, Gly), 173.2 (CO, Glu), 173.5 (CO,

Pro), 173.8 (CO, Hyp), 174.3 (CO, Hyp), 174.5 (COOH, Glu), 177.0 (COOH, Gly). HRMS (ESI-MS, m/z) ($M + H$)⁺ calc. for C₃₆H₆₁N₁₀O₁₃: 841.4420, found: 841.4424.

5.2.4. Synthesis of the α -triple-helix monomer peptide (**8**)

Synthesis of peptide **8** started from commercially available Fmoc(9-fluorophenylmethoxy)-Cys(Trt)-Sasrin® (271.76 mg, 0.106 mmol). The completed peptide was cleaved from the resin and side chain deprotected by treatment with the scavengers water/thioanisole/triisopropylsilane/dichloromethane/trifluoroacetic acid (1:1:1:10:20 v/v) for 4 h at room temperature. The solid support was removed by filtration, the filtrate concentrated under reduced pressure, and the peptide **8** precipitated from diethyl ether. Precipitate was washed several times with diethyl ether and dried under reduced pressure. Peptide **8** was purified using reverse-phase chromatography and the composition verified by spectrometric analysis. Peptide **8** was obtained as a white powder (171.22 mg, 41.7%). IR (cm⁻¹): 3280 (NH, NH₂, OH), 3070 (CH), 1680 (CO), 1651 (CO). HRMS (ESI-MS, m/z) ($M + H$)⁺ calc. for C₁₇₆H₂₆₀N₄₆O₄₉S₂: 3865.8709, found: 3865.8656.

5.3. Structural studies

5.3.1. Circular dichroism

Circular dichroism (CD) measurement was carried out in the far UV (250–190 nm) on a Jobin yvon CD6 (UMR CNRS/USTL 8576-IFR 118, Lille, France) spectropolarimeter. The spectra recorded with a 0.1–1 cm optical path length of the quartz cell, with five replicates at a scan rate of 0.5 nm/min. The CD data were expressed in terms of mean residue ellipticity ($[\theta]$) in deg cm² dmol⁻¹. The concentrations for CD analysis were 1 mg/mL in 0.5 M acetic acid or in the mixture of methanol and acetic acid (85/15). The CD spectra of all the samples were scanned after 7-day storage at 4 °C. All CD spectra measured were baseline corrected subtracting by the buffer spectrum. The P_{II} helix content, for the peptides **6–8**, was determined by using this equation [21]:

$$\%PP_{II} = \frac{[\theta]_{\max} + 6100}{13,700} \times 100$$

The thermal transition curves were obtained by recording the molar ellipticity ($[\theta]$) in the range of 4–60 °C at $\lambda = 225$ nm at a rate of 12 °C/h. The fraction folded was calculated from CD melting curves as

$$F = \frac{\theta_{\text{obs}} - \theta_{\text{monomer}}}{\theta_{\text{trimer}} - \theta_{\text{monomer}}}$$

where θ_{obs} is the observed ellipticity, θ_{trimer} is the ellipticity when the peptide is fully associated, and θ_{monomer} is the ellipticity of the monomer. The values for these ellipticities were determined in accordance with the method developed by Brodsky [19]. The melting temperature (T_m) was obtained as a midpoint of the transition, that is, $F(T_m) = 1/2$.

5.3.2. Calculation of thermodynamic parameters

The thermodynamic data was determined by using the van't Hoff analysis. The melting curves were analyzed using a two-state model, where three unfolded chains combine to form a triple helix [18,19,23,24]:



The equilibrium constant and Gibb's energy were determined from the equilibrium melting experiment (c is the monomeric peptide concentration in moles and F is the fraction folded) as:

$$K = \frac{[U]^3}{[N]} = \frac{3c^2(1-F)^3}{F}$$

$$\Delta G = -RT \ln K$$

$$\Delta H = 8RT_m^2(\delta\alpha/\delta T)_{T=T_m}$$

The van't Hoff enthalpy ΔH was determined by curve fitting with the equation and the following equation was used to calculate ΔS . Peptide **6**:

$$K = \exp[\Delta H/RT(T/T_m - 1)] \quad \Delta S = \Delta H/T_m$$

Peptides **5**, **7**, **8**:

$$K = \exp\left[\frac{\Delta H}{RT(T/T_m - 1)} - \ln(0.75c^2)\right] \Delta S \\ = \Delta H/T_m - \ln(0.75c^2)$$

The following equation was used to calculate ΔG :

$$\Delta G = \Delta H - T\Delta S$$

The ΔG values were calculated at the average melting temperatures ($T = 310.4$ K) to minimize the extrapolation of the temperature dependence of ΔH and ΔS .

Acknowledgment

We are grateful to Gérard Montagne (UMR CNRS/USTL 8576-IFR 118, Lille, F-59655 France) for obtaining the CD spectra. This work was supported by INSERM and a grant from the "programme inter-regional: Régulation de la Matrice Extracellulaire et Pathologies" no. R03007HH. Viviane Pires was the recipient of a grant from the CNPq (Brazil).

References

- [1] (a) A. Rich, F.H.C. Crick, J. Mol. Biol. 3 (1961) 483–506; (b) J. Bella, M. Eaton, B. Brodsky, H. Berman, Science 266 (1994) 75–81; (c) J. Baum, B. Brodsky, Folding of the Collagen Triple-helix and Its Naturally Occurring Mutants, in: R.H. Pain (Ed.), Mechanisms of Protein Folding, second ed., Oxford University Press, 2000, pp. 330–351; (d) B. Brodsky, A.V. Persikov (Eds.), Molecular Structure of the Collagen Triple Helix, Advances in Protein Chemistry, vol. 70, Elsevier Inc., 2005, pp. 301–339.
- [2] (a) C.M. Kielty, M.E. Grant, The Collagen Family: Structure, Assembly, and Organization in the Extracellular Matrix, in: P.M. Royce, B. Steinmann (Eds.), Connective Tissue and its Heritable Disorders, Wiley, 2002, pp. 159–222; (b) C.G. Fields, C.M. Lovdahl, A.J. Miles, V.L.M. Hagen, G.B. Fields, Biopolymers 33 (1993) 1695–1707.
- [3] (a) H.R. Baumgartner, T.B. Tschopp, H.J. Weiss, Thromb. Haemost. 37 (1977) 17–28; (b) J. Rautenberg, E. Jaeger, M. Althaus, Curr. Top. Pathol. 87 (1993) 163–192.
- [4] (a) J. Chen, T.G. Diacovo, D.G. Grenache, S.A. Santoro, M.M. Zutter, Am. J. Pathol. 161 (2002) 337–344; (b) L. He, L.K. Pappan, D.G. Grenache, Z. Li, D.M. Tollefsen, S.A. Santoro, M.M. Zutter, Blood 102 (2003) 3652–3657.
- [5] (a) R.W. Farndale, J.J. Sixma, M.J. Barnes, P.G. de Groot, J. Thromb. Haemost. 2 (2004) 561–573; (b) N. Raynal, S.W. Hamaia, P.R.-M. Siljander, B. Maddox, A.R. Peachey, R. Fernandez, L.J. Foley, D.A. Slatyer, G.E. Jarvis, R.W. Farndale, J. Biol. Chem. 281 (2006) 3821–3831; (c) R.W. Farndale, D.A. Slatyer, P.R.-M. Siljander, G.E. Jarvis, J. Thromb. Haemost. 5 (2007) 220–229.
- [6] (a) E. Monnet, F. Fauvel-Lafève, J. Biol. Chem. 275 (2000) 10912–10917; (b) P. Maurice, L. Waeckel, V. Pires, P. Sonnet, M. Lemesle, B. Arbeille, J. Vassy, J. Rochette, C. Legrand, F. Fauvel-Lafève, Histochem. Cell. Biol. 125 (2006) 407–417.
- [7] A. Karniguian, Y.J. Legrand, P. Lefrancier, J.P. Caen, Thromb. Res. 32 (1983) 593–604.
- [8] P. Maurice, V. Pires, C. Amant, A. Kauskot, S. Da Nascimento, P. Sonnet, J. Rochette, C. Legrand, F. Fauvel-Lafève, A. Bonnefoy, Vasc. Pharmacol. 44 (2006) 42–49.
- [9] V. Pires, J. Pêcher, S. Da Nascimento, P. Maurice, A. Bonnefoy, A. Dassonville, C. Amant, F. Fauvel-Lafève, C. Legrand, J. Rochette, P. Sonnet, Eur. J. Med. Chem. 42 (2007) 694–701.
- [10] P.R. Erickson, M.C. Herzberg, G. Tierney, J. Biol. Chem. 267 (1992) 10018–10023.

- [11] (a) C.G. Fields, D.J. Mickelson, S.L. Drake, J.B. McCarthy, G.B. Fields, *J. Biol. Chem.* 268 (1993) 14153–14160;
(b) S. Sakakibara, Y. Kishida, Y. Kikuchi, R. Sakai, K. Kakiuchi, *Bull. Chem. Soc. Jpn.* 41 (1968) 1273–1275.
- [12] (a) C.G. Knight, L.F. Morton, D.J. Onley, A.R. Peachey, T. Ichinohe, M. Okuma, R.W. Farndale, M.J. Barnes, *Cardiovasc. Res.* 41 (1999) 450–457;
(b) B. Kehrel, S. Wierwille, K.J. Clemetson, O. Anders, M. Steiner, C.G. Knight, R.W. Farndale, M. Okuma, M.J. Barnes, *Blood* 91 (1998) 491–499.
- [13] R.W. Woody, B. Brodsky, *Adv. Biophys. Chem.* 2 (1992) 37–79.
- [14] R.W. Woody, in: K. Nakanishi, N. Berova, R.W. Woody (Eds.), *Circular Dichroism: Principles and Applications*, VCH, New York, 1994, pp. 473–496.
- [15] W. Engel, T. Vogl, W. Voelter, C. Urbanke, D. Scheulder, J. Rauterberg, *Biochemistry* 38 (1999) 13610–13622.
- [16] S.J. Whittington, B.W. Chellgren, V.M. Hermann, T.P. Creamer, *Biochemistry* 44 (2005) 6269–6275.
- [17] Y. Feng, G. Melacini, J.P. Taulane, M. Goodman, *J. Am. Chem. Soc.* 118 (1996) 10351–10358.
- [18] (a) A.V. Persikov, Y. Xu, B. Brodsky, *Protein Sci.* 13 (2004) 893–902;
(b) Y. Nishi, S. Uchiyama, M. Doi, Y. Nishiuchi, T. Nakazawa, T. Ohkubo, Y. Kobayashi, *Biochemistry* 44 (2005) 6034–6042.
- [19] N.K. Shah, J.A.M. Ramshaw, A. Kirkpatrick, C. Shah, B. Brodsky, *Biochemistry* 35 (1996) 10262–10268.
- [20] B.J. Stapley, T.P. Creamer, *Protein Sci.* 8 (1999) 587–595.
- [21] M.A. Kelly, B.W. Chellgren, A.L. Rucker, J.M. Troutman, M.G. Fried, A.-F. Miller, T.P. Creamer, *Biochemistry* 40 (2001) 14376–14383.
- [22] R. Aurora, T.P. Creamer, R. Srinivasan, G.D. Rose, *J. Biol. Chem.* 272 (1997) 1413–1416.
- [23] A.V. Persikov, J.A.M. Ramshaw, A. Kirkpatrick, B. Brodsky, *J. Mol. Biol.* 316 (2002) 385–394.
- [24] (a) J. Engel, H.T. Chen, D.J. Prockop, H. Klump, *Biopolymers* 16 (1977) 601–622;
(b) L.A. Marky, K.J. Breslauer, *Biopolymers* 26 (1987) 1601–1620.